

Density functionals and dimensional renormalization for an exactly solvable model

S. Kais and D. R. Herschbach

Department of Chemistry, Harvard University, Cambridge, Massachusetts 02138

N. C. Handy, C. W. Murray, and G. J. Laming

University Chemical Laboratory, Lensfield Road, Cambridge, CB2 1EW, United Kingdom

(Received 22 January 1993; accepted 24 March 1993)

We treat an analytically solvable version of the “Hooke’s Law” model for a two-electron atom, in which the electron–electron repulsion is Coulombic but the electron-nucleus attraction is replaced by a harmonic oscillator potential. Exact expressions are obtained for the ground-state wave function and electron density, the Hartree–Fock solution, the correlation energy, the Kohn–Sham orbital, and, by inversion, the exchange and correlation functionals. These functionals pertain to the “intermediate” density regime ($r_s \gtrsim 1.4$) for an electron gas. As a test of customary approximations employed in density functional theory, we compare our exact density, exchange, and correlation potentials and energies with results from two approximations. These use Becke’s exchange functional and either the Lee–Yang–Parr or the Perdew correlation functional. Both approximations yield rather good results for the density and the exchange and correlation energies, but both deviate markedly from the exact exchange and correlation potentials. We also compare properties of the Hooke’s Law model with those of two-electron atoms, including the large dimension limit. A renormalization procedure applied to this very simple limit yields correlation energies as good as those obtained from the approximate functionals, for both the model and actual atoms.

I. INTRODUCTION

Electronic structure calculations at present rely chiefly on the Hartree–Fock (HF) self-consistent field approximation, augmented by configuration interaction (CI). Although HF calculations usually give good total energies, the error in the HF approximation—termed the correlation energy—is typically comparable to or larger than bond dissociation energies. For instance, in the case of the fluorine molecule, the HF approximation gives better than 99.6% of the total energy, yet fails to predict that the molecule is bound.¹ Even elaborate CI calculations often are not sufficient to distinguish reliably among variant molecular geometries or reaction pathways. Evaluating the correlation energy thus remains a major problem for *ab initio* quantum chemistry.²

Density functional theory^{3–6} offers another approach, much simpler to implement and interpret than the CI method. The formulation employing the Kohn–Sham (KS) equations⁷ involves single particle orbitals, as in the HF method, so entirely avoids CI calculations. In principle, the KS method can yield exact results for the energy and electron density, but in practice the accuracy is limited because the correct form of the exchange–correlation functional is not known. Here we treat a two-electron model problem for which this functional can be determined exactly. Our purpose is to test approximate functionals that are often used in the KS method and to examine how the exactly solvable large dimension limit⁸ might be utilized to improve the treatment of correlation.

We consider the “Hooke’s Law” (HL) atom, in which the electron-nucleus attraction is replaced by an harmonic oscillator potential but the electron–electron repulsion re-

mains Coulombic. Several authors have previously treated this or kindred models in order to study aspects of electron correlation.^{9–14} Most pertinent is the work of Laufer and Krieger.¹² They provided extensive numerical calculations for the HL model for a wide range of the harmonic oscillator spring constant and found that KS exchange and correlation energies obtained from the frequently used local-density approximation and some variants are significantly in error.

In Sec. II we obtain an exact expression for the ground-state electron density for a HL model with a particular value of the spring constant that permits an analytical solution to be derived from supersymmetry.¹⁴ In Sec. III we evaluate the corresponding Hartree–Fock approximation and the correlation energy. In Sec. IV we construct the exact KS solution for the $1s^2$ spin-paired configuration, by inversion derive the exchange and correlation potentials and functionals, and compare with approximate functionals. In Sec. V we evaluate the correlation energy by applying a renormalization procedure to the large dimension limit.⁸ In Sec. VI inferences from the HL model are noted that suggest means to improve approximations for the exchange and correlation functionals of actual atoms, particularly by employing dimensional scaling.

II. HOOKE’S LAW MODEL

For the HL atom the Hamiltonian in bohr-hartree atomic units ($\hbar = m = e = 1$) is

$$H = -\frac{1}{2}(\nabla_1^2 + \nabla_2^2) + \frac{1}{2}k(r_1^2 + r_2^2) + \frac{1}{r_{12}}, \quad (1)$$

where k is the oscillator spring constant, r_1 and r_2 the distances of the electrons from the nucleus, and $\mathbf{r}_{12} = |\mathbf{r}_1 - \mathbf{r}_2|$ the distance between each other. In terms of the centroid coordinate, $\mathbf{R} = \frac{1}{2}(\mathbf{r}_1 + \mathbf{r}_2)$, and $\mathbf{r} = (\mathbf{r}_1 - \mathbf{r}_2)$, the Hamiltonian becomes separable; thus

$$(-\frac{1}{4}\nabla_{\mathbf{R}}^2 + kR^2)\chi(\mathbf{R}) = E_R\chi(\mathbf{R}), \quad (2)$$

$$\left(-\nabla_{\mathbf{r}}^2 + \frac{1}{4}kr^2 + \frac{1}{r}\right)\Phi(\mathbf{r}) = E_r\Phi(\mathbf{r}), \quad (3)$$

where the total wave function is given by $\Psi(\mathbf{r}_1, \mathbf{r}_2) = \chi(\mathbf{R})\phi(\mathbf{r})$ and the total energy by $E = E_R + E_r$. As shown in a previous study,¹⁴ for the particular value $k = \frac{1}{4}$, the ground-state solution can be obtained analytically as

$$\Psi(r_1, r_2) = N_0(1 + \frac{1}{2}r_{12})e^{-(1/4)(r_1^2 + r_2^2)} \quad (4)$$

with

$$E = E_R + E_r = \frac{3}{4} + \frac{5}{4} = 2 \quad (5)$$

and N_0 the normalization constant. The exact single-particle density thus is given by

$$\rho(r_1) = 2 \int |\Psi(\mathbf{r}_1, \mathbf{r}_2)|^2 d\mathbf{r}. \quad (6)$$

On evaluating the integral we obtain

$$\rho(r) = 2N_0^2 e^{-(1/2)r^2} \left\{ \left(\frac{\pi}{2}\right)^{1/2} \left[\frac{7}{4} + \frac{1}{4}r^2 + \left(r + \frac{1}{r}\right) \operatorname{erf}(2^{-1/2}r) \right] + e^{-(1/2)r^2} \right\}, \quad (7)$$

where $r \equiv r_1$ and erf denotes the error function. The normalization constant is obtained from the condition $\int \rho(\mathbf{r}) d\mathbf{r} = 2$, which gives

$$N_0^2 = \pi^{3/2} (8 + 5\pi^{1/2})^{-1}. \quad (8)$$

Figure 1 plots the density $\rho(r)$ and $r^2\rho(r)$ for our HL model (with $k = \frac{1}{4}$) and for the He atom.¹⁵ At the origin, the HL density is finite and has zero slope; at large r the density is dominated by the e^{-r^2} factor in Eq. (7). The He density is also finite at the origin but is quite large there and has nonzero slope; at large r it decays as e^{-r} . These features directly reflect the different attractive forces. Also included in Fig. 1 (as dotted curves) are the densities $\rho_0(r)$ obtained by omitting the electron-electron repulsion and thereby entirely removing electron correlation. For both the HL model and He, electron-electron repulsion increases the density at large distances and decreases it near the nucleus.^{12,13}

III. HARTREE-FOCK SOLUTION

The HF equation corresponding to the HL model is^{11,13}

$$\left\{-\frac{1}{2}\nabla^2 + v_{\text{ext}}(r) + v_H[\rho_{\text{HF}}(r)]\right\}\phi_{\text{HF}}(r) = \epsilon_{\text{HF}}\phi_{\text{HF}}(r), \quad (9)$$

where $r \equiv r_1$ (or r_2), the external potential $v_{\text{ext}} = \frac{1}{2}kr^2$, and the Hartree or Coulomb potential is defined as

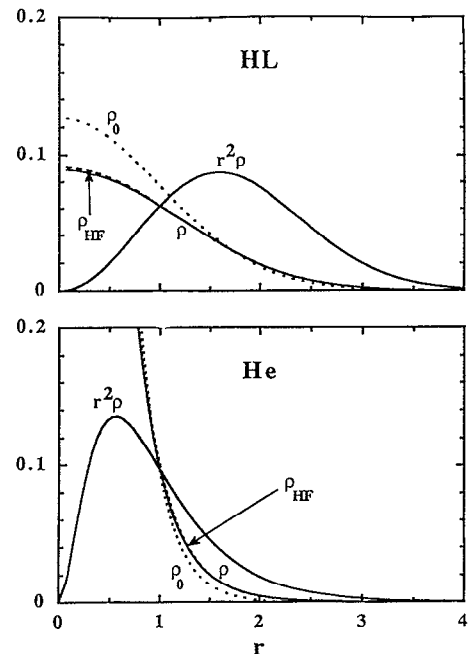


FIG. 1. Single-electron density distributions $\rho(r)$ and $r^2\rho(r)$ for He atom and the Hooke's Law model (exact solution for $\frac{1}{4}$). Solid curves are for the complete Hamiltonian; dashed curves for the Hartree-Fock version. Dotted curves omit the $1/r_{12}$ electron-electron repulsion term, thus correspond to $\rho_0(r) = 2(Z^3/\pi)\exp(-2Zr)$ for the atom and to $2(\omega_0/\pi)^{3/2}\exp(-\omega_0 r^2)$ for the HL model, with $\omega_0 = k^{1/2}$. Distributions normalized such that $4\pi \int_0^\infty r^2 \rho dr = 2$.

$$v_H[\rho(r)] \equiv \frac{1}{2} \int \frac{\rho(r')}{|\mathbf{r} - \mathbf{r}'|} dr'. \quad (10)$$

The total $1s^2$ variational wavefunction is $\Psi(r_1, r_2) = \phi(r_1)\phi(r_2)$ and ϵ_{HF} is the orbital energy. A self-consistent solution of Eq. (9) yields the HF density

$$\rho_{\text{HF}}(r) = 2|\phi(r)|^2 \quad (11)$$

and the total energy

$$E_{\text{HF}} = 2\epsilon_{\text{HF}} - \frac{1}{2} \int \rho_{\text{HF}}(\mathbf{r}) v_H[\rho_{\text{HF}}(\mathbf{r})] d\mathbf{r}. \quad (12)$$

Numerical solutions are readily obtained from a standard HF code¹⁶ by simply replacing the Coulombic attraction $-1/r$ by $\frac{1}{2}kr^2$. For $k = \frac{1}{4}$, we find $\epsilon_{\text{HF}} = 1.27713$ and $E_{\text{HF}} = 2.039325$. Subtracting E_{HF} from Eq. (5) gives the correlation energy as -0.039325 , or 1.97% of the total energy. This value is remarkably close to the $1s^2$ correlation energies of actual two-electron atoms; e.g., -0.042044 or 1.45% for helium.

Figure 1 includes (as dashed curves) the HF density $\rho_{\text{HF}}(r)$ for both the HL model and the He atom. The deviations from the exact density are barely discernable on this scale.

IV. KOHN-SHAM FUNCTIONALS

Like the HF equations, the KS formalism⁷ involves single-particle orbitals describing noninteracting electrons moving in a local effective potential. In principle, however,

the KS equations can give the exact ground state electron density and energy of the interacting system. In practice, this is frustrated by the lack of a means to construct the correct exchange-correlation energy, a universal functional of $\rho(r)$. For the ground state of the HL model, the exact KS solution can readily be obtained and inverted¹² to derive the exchange and correlation potentials.

A. Inversion procedure

The KS equation for the HL model is

$$(-\frac{1}{2}\nabla^2 + v_{\text{eff}}[\rho(\mathbf{r})])\phi(\mathbf{r}) = \epsilon_i \phi_i(\mathbf{r}) \quad (13)$$

where $\mathbf{r} \equiv \mathbf{r}_i$ ($i=1,2$) and the effective potential is

$$v_{\text{eff}}[\rho(\mathbf{r})] = v_{\text{ext}}(\mathbf{r}) + 2v_H[\rho(\mathbf{r})] + v_{\text{xc}}[\rho(\mathbf{r})] \quad (14)$$

with $v_{\text{xc}}[\rho(\mathbf{r})] = \delta E_{\text{xc}}[\rho]/\delta\rho$ the exchange-correlation potential, the functional derivative of the exchange-correlation energy. For two electrons of opposite spin, the KS single-orbital wave function $\phi_i \equiv \phi_{\text{KS}}$ and energy $\epsilon_i \equiv \epsilon_{\text{KS}}$ are the same. The electron density is simply given by

$$\rho(\mathbf{r}) = 2|\phi_{\text{KS}}(\mathbf{r})|^2 \quad (15)$$

and this is identically equal to the density of the interacting two-electron system. The total energy is given by

$$E = 2\epsilon_{\text{KS}} - \int \rho v_H[\rho] d\mathbf{r} - \int \rho v_{\text{xc}}[\rho] d\mathbf{r} + E_{\text{xc}}[\rho]. \quad (16)$$

These KS equations are only exact if the $E_{\text{xc}}[\rho]$ and $v_{\text{xc}}[\rho]$ functionals used are exact.

For the HL model we can invert Eq. (15) to obtain the exact KS orbital (analytically for $k=\frac{1}{4}$) via $\phi_{\text{KS}}(\mathbf{r}) = [\frac{1}{2}\rho(\mathbf{r})]^{1/2}$, since the orbital wave function can be taken as real and Eq. (6) provides the exact density. This enables us to invert Eq. (13) to obtain the exchange-correlation functional from

$$v_{\text{xc}}[\rho] = \epsilon_{\text{KS}} - v_{\text{ext}}(\mathbf{r}) - 2v_H[\rho] - v_{\text{KE}}[\rho], \quad (17)$$

where the last term comes from the kinetic energy,

$$v_{\text{KE}}[\rho] \equiv -\frac{1}{2} \frac{\nabla^2 \phi}{\phi} = \frac{1}{4} \left(\frac{\nabla^2 \rho}{\rho} \right) - \frac{1}{8} \left(\frac{\nabla \rho}{\rho} \right)^2. \quad (18)$$

Likewise, we can invert Eq. (16) to determine the $E_{\text{xc}}[\rho]$ functional. The orbital energy ϵ_{KS} may be determined without actually solving the KS equation. This can be done by exploiting the limit $r \rightarrow \infty$, by virtue of the condition that v_{xc} and the Coulomb integral in Eq. (17) vanish in that limit.¹² For $k=\frac{1}{4}$, we find by computing the asymptotic values of $\nabla^2 \rho/\rho$ and $\nabla \rho/\rho$ from Eq. (7) that

$$\epsilon_{\text{KS}} = \lim_{r \rightarrow \infty} [\frac{1}{2}kr^2 - \frac{1}{4}(r^2 - 7) + \frac{1}{8}(r^2 - 4)] = \frac{5}{4}. \quad (19)$$

Thus $\epsilon_{\text{KS}} = E_r$, the eigenvalue obtained in Eq. (5) for relative motion of the electrons; this result in fact holds generally for the HL model¹² (with any $k > 0$). The orbital energy can also be determined from a quite general theo-

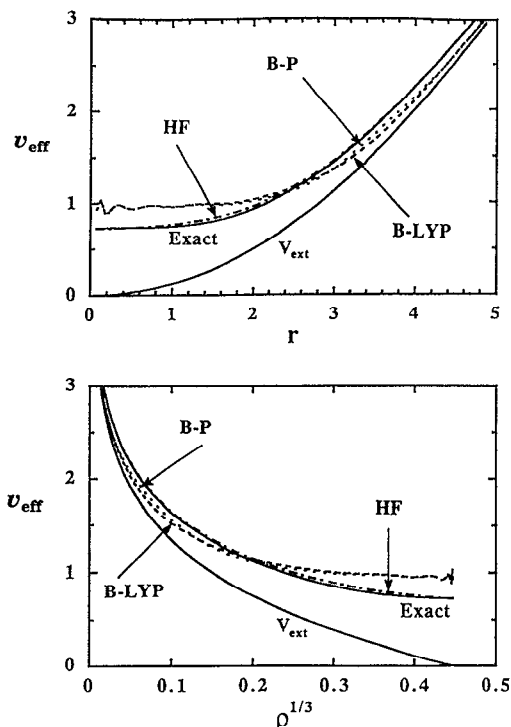


FIG. 2. Effective single-particle potential v_{eff} of Eq. (14) for the HL model ($k=\frac{1}{4}$) as function of r and ρ . Solid curves are exact results, others approximate; dashed curves from BLYP; dotted curves from BP; dotted-dashed from HF. In each case, the potential is evaluated with the corresponding density. Also shown is an exact curve for the external term alone, $v_{\text{ext}} = \frac{1}{2}kr^2$.

rem¹⁷ stating that ϵ_{KS} for the highest occupied orbital is the difference in total energies for systems with N and $(N-1)$ particles,

$$(\epsilon_{\text{KS}})_{\text{max}} = E(N) - E(N-1). \quad (20)$$

The HL model has only one occupied orbital, and for $k=\frac{1}{4}$, we have $E(2)=2$ and $E(1) = \frac{3}{2}k^{1/2} = \frac{3}{4}$. For this case, the KS result differs from the HF orbital energy by only -2.2% .

B. Exchange and correlation potentials

Figures 2–4 display (as solid curves) exact potentials derived by inverting the KS equations. In Fig. 2, we show the total effective potential v_{eff} and also v_{ext} . In Figs. 3 and 4 we show the components of the exchange-correlation potential, $v_{\text{xc}} = v_x + v_c$, as functions of both r and ρ . For two electrons of opposite spin, the exact exchange component is just the negative of the Coulomb potential,

$$v_x[\rho] = -v_H[\rho]. \quad (21)$$

The exact correlation potential is then given by

$$v_c[\rho] = v_{\text{xc}}[\rho] - v_x[\rho]. \quad (22)$$

These potentials are readily evaluated using ρ from Eq. (7).

Note that with these relations Eq. (14) may be recast as

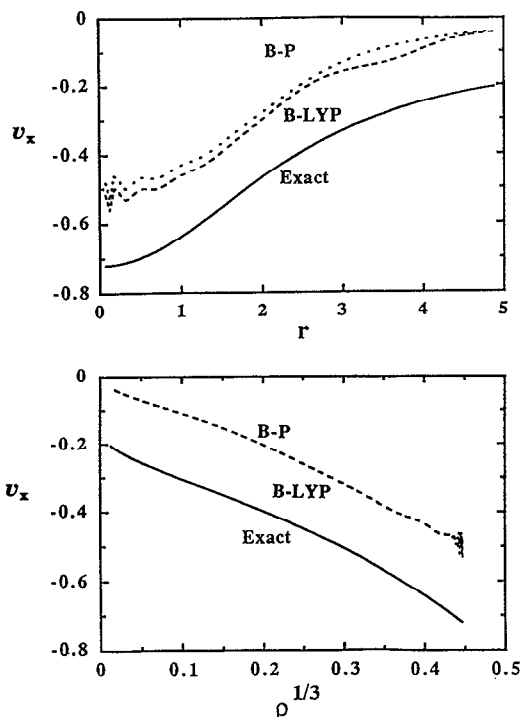


FIG. 3. Exchange potential v_x of Eq. (21) for the HL model ($k=\frac{1}{4}$). Notation as in Fig. 2.

$$v_{\text{eff}}[\rho] = v_{\text{ext}}(r) + v_H[\rho] + v_c[\rho]. \quad (23)$$

Thus, for a $1s^2$ system, v_{eff} for the KS equation differs from that for the HF equation simply by addition of the corre-

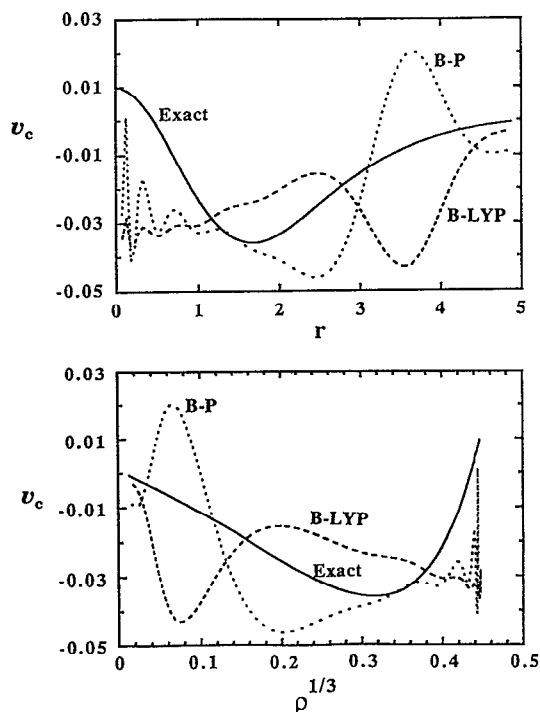


FIG. 4. Correlation potential v_c of Eq. (22) for the HL model ($k=\frac{1}{4}$). Notation as in Fig. 2.

TABLE I. Potential functionals for HL model. Derived from Eqs. (21) and (22) for Hooke's Law model ($k=\frac{1}{4}$). Tabulated quantities are coefficients a_n in a polynomial fit, $v = \sum_n a_n x^n$, with $x = \rho^{1/3}$; the least-squares $R=0.9999$

Order	v_x	v_c
0	-0.1864	0.0003
1	-1.6883	-0.0785
2	7.7938	-0.7486
3	-34.263	4.7809
4	65.921	-15.910
5	-50.985	22.536

lation potential, with all terms evaluated for the exact $\rho(r)$ rather than the HF density. Figure 2 includes (dotted-dashed curve) the HF version of v_{eff} , evaluated with $\rho_{\text{HF}}(r)$; this differs only slightly from the exact potential.

Figures 2–4 also include comparisons (dashed and dotted curves) with two approximations frequently used in current density functional calculations.¹⁸ One approximation, designated Becke–Lee–Yang–Parr (BLYP), employs the Dirac form for the exchange energy with Becke's 1988 gradient exchange correction,¹⁹ and obtains the correlation energy from Lee, Yang, and Parr's functional that involves a second-order gradient expansion based on the HF density matrix.¹⁹ A correlation factor is included which contains four parameters that were fitted to the HF density for the helium atom.²⁰ The other approximation, designated as Becke–Perdew (BP), treats the exchange energy the same way but derives the correlation energy from an interpolation²¹ of Monte Carlo results.²² This is augmented by a nonlocal correction²³ that improves a generalized gradient expansion.²⁴ For our comparisons, we employed the BLYP and BP functionals in the KS equation of Eq. (13), derived the corresponding densities and eigenvalues by a self-consistent solution,¹⁸ and with these evaluated the potentials and energies.

As functions of r , the effective potentials v_{eff} for the BLYP and BP approximations are quite similar, but lie substantially above the exact potential at small r and below at large r . For the exchange potential v_x , the approximations lie well above the exact potential at all r ; furthermore, although the approximations nearly coincide (at the scale shown), spurious oscillations appear for $r < 1.5$. As seen in Fig. 1, this region lies inside the maximum in $r^2\rho(r)$ for the HL model. For the correlation potential v_c , which is much smaller, the spurious oscillations are greatly magnified. The deviations from the exact potential differ markedly for BLYP and BP but are of comparable size and fluctuating sign. Curiously, these deviations are roughly out of phase for $r > 1$ but in phase at shorter distances, where both approximations underestimate the correlation potential.

As functions of ρ , the potentials display the same features. However, as seen in Fig. 1, for the HL model the transformation $r \rightarrow \rho$ maps the abscissa scale into a finite range. The BLYP and BP approximations give quite similar $v_{\text{eff}}(r)$ and $v_x(r)$ functions. The exact $v_x(r)$ and $v_c(r)$ are smooth functions that can be well represented by a

TABLE II. Energy terms for Hooke's Law model ($k=\frac{1}{4}$).

Case	E	E_{KE}	E_{ext}	E_H	E_x	E_c
Exact KS	2.0000	0.6352	0.8881	0.5160	-0.516	-0.0393
BLYP	2.0172	0.6313	0.8933	0.5146	-0.5016	-0.0351
BP	1.9985	0.6327	0.8926	0.5141	-0.5012	-0.0538
HF	2.0392	0.6318	0.8925	0.5150	-0.5150	0

fifth-order polynomial in $\rho^{1/3}$. Table I lists the coefficients.

C. Exchange and correlation energies

We can determine the exact $E_{xc}[\rho]$ by recasting Eq. (16) for the total energy by use of Eq. (17) and obtain

$$E = E_{ext} + E_{KE} + 2E_H + E_{xc}, \quad (24)$$

where

$$E_{ext}[\rho] = \int \rho(r) v_{ext}(r) dr, \quad (25)$$

$$E_{KE}[\rho] = \int \rho(-\frac{1}{2} \nabla^2 \phi / \phi) dr, \quad (26)$$

and

$$E_H[\rho] = \frac{1}{2} \int \rho v_H[\rho] dr = -E_x[\rho], \quad (27)$$

since by virtue of Eq. (21) the exact exchange energy is the negative of the Hartree energy. The exact correlation energy thus can be determined from

$$E_c[\rho] = E_{xc}[\rho] - E_x[\rho]. \quad (28)$$

In evaluating the corresponding energy terms for the BLYP and BP approximations, we use the customary formulas^{19,23} aside from introducing for v_{ext} the oscillator form.

Table II compares values of the total energy and the contributing terms: external, kinetic energy, Coulomb, exchange, and correlation. The BLYP and BP approximations both give good total energies (in error by +0.87% and -0.08%, respectively, substantially better than the HF result (in error by +1.97%). However, the exchange energies (in error by 2.79% and 2.86%) are much less accurate than the HF value (in error by only 0.02%), whereas the correlation energies are relatively good (in error by -11% and +27%). The top row in Table II gives the exact KS results. We note that the expectation value of the kinetic energy, $-\frac{1}{2}(\nabla_1^2 + \nabla_2^2)$, computed with the exact wave function of Eq. (4) is 0.6644; this exceeds the KS kinetic energy, in accord with a general theorem.^{5,7} The increment of 0.0292 is comparable to the correlation energy and quite similar to two-electron atom (TEA) values (cf. Ref. 5, Table 7.1): 0.029, 0.037, and 0.040 for $Z=1, 2$, and 3, respectively.

These results as well as the BLYP and BP potentials of Figs. 2-4 are appreciably better, especially for correlation, than those given by the approximate functionals examined by Laufer and Krieger.¹² However, our comparisons indi-

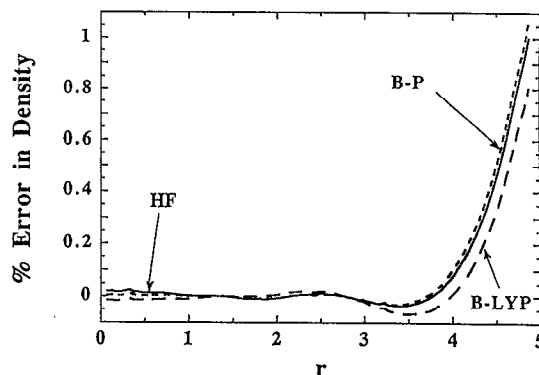


FIG. 5. Comparison of single-electron density functions for the HL model ($k=\frac{1}{4}$) as obtained from the HF (solid curve), BLYP (dashed curve), and BP (dotted curve) approximations. Ordinate gives the difference between the approximate and exact density divided by the exact density, the latter given by Eq. (7).

cate the same conclusions. (1) The potential functionals (as shown in Figs. 2-4) provide a much more incisive test of an approximate exchange-correlation functional than do energies, especially the total energy. (2) In density functional theory, current approximations for exchange introduce substantially larger absolute errors than for correlation.

Figure 5 complements Table II and Fig. 2 by comparing the deviations from the exact density for the HF, BLYP, and BP approximations. Except for $r > 4$, where the density becomes quite small, the deviations are only a few percent. The effect of including correlation in the BLYP and BP approximations is evident only at small r , where both give slightly lower density than the HF approximation. These comparisons emphasize an ironic situation, especially apparent in the v_{eff} functions of Fig. 2. The HF approximation treats exchange well but lacks correlation. The BLYP and BP methods include correlation and obtain better total energies, but the exchange and correlation potentials are both inaccurate and the corresponding v_{eff} functions differ much more from the exact result than does the HF version.

V. LARGE DIMENSION LIMIT

Another strategy for treating correlation is suggested by recent applications of dimensional scaling to electronic structure.⁸ This involves generalizing the problem to D dimensions and introducing scale factors to remove the major, generic D dependence. Often such scaled quantities can be easily evaluated for the $D \rightarrow \infty$ limit or other special values and used to construct an approximation for $D=3$. Among recent applications is a dimensional interpolation treatment of a hard-sphere fluid,²⁵ analogous to interpolation between the low and high density limits for an electron gas.²⁶ For the He atom, the large dimension limit was found^{27,28} to account for 64% of the correlation energy for $D=3$ and this estimate was recently improved to 98% by means of a simple charge renormalization procedure.⁸ Here we outline similar calculations for the HL model.

TABLE III. Large D limit [results for HL model ($k=\frac{1}{4}$) from Eq. (30), for He atom from Refs. 27 and 28].

	HL model		He atom	
	Exact	HF	Exact	HF
r_m	1.898 35	1.8999	1.213 93	1.214 74
θ_m	99.644°	90°	95.301°	90°
E_∞	2.0684	2.08401	-2.737 81	-2.710 79
$E_c(D=\infty)$	-0.023 61		-0.026 98	
$E_c(D=3)$	-0.0392		-0.042 044	

Because the potential energy in Eq. (1) for the HL model is not a homogeneous function of the radial coordinates, as is the Coulombic potential for atoms, the scaling procedure must be modified. We use a method recently detailed by López-Cabrera, Tan, and Loeser.²⁹ The resulting D -scaled Hamiltonian has the same form as the $D=3$ Hamiltonian of Eq. (1), with three net changes: insertion of a factor of $(3/D)^2$ in front of the Laplacian operators, a factor of $(3/D)[(D-1)/2]$ in front of the $1/r_{12}$ Coulombic term, and addition of a centrifugal term³⁰ given by

$$\left(\frac{3}{D}\right)^2 \left(\frac{D-3}{2}\right)^2 \left[\frac{1}{2} \left(\frac{1}{r_1^2} + \frac{1}{r_2^2} \right) \frac{1}{\sin^2 \theta} \right], \quad (29)$$

where θ is the angle between r_1 and r_2 , the electron-nucleus radii. In the $D \rightarrow \infty$ limit, the Laplacian terms are quenched. The scaled energy in this limit is then found simply by minimizing an effective potential, $W(r_1, r_2, \theta)$. This is comprised of the centrifugal term, the repulsive Coulombic term, and the attractive oscillator potential. The minimum occurs for a symmetric configuration, with $r_1 = r_2$. The energy and electronic geometry for $D \rightarrow \infty$ thus are obtained from $E_{\min} = \min W(r, r, \theta)$, with

$$W = \left(\frac{3}{2}\right)^2 (r \sin \theta)^{-2} + kr^2 + \left(\frac{3}{2}\right) [2^{1/2} r (1 - \cos \theta)]^{-1/2}. \quad (30)$$

The large dimension limit for the HF approximation²⁸ is obtained by merely imposing the constraint $\theta = 90^\circ$. Thus, in this limit, elementary calculations yield the exact correlation energy.

Table III gives the large D limit found for the $k=\frac{1}{4}$ case, together with corresponding results for the He atom. The correlation energy for the HL model at $D \rightarrow \infty$ is about 60% of that for $D=3$ (compared with 64% for the He atom). Figure 6 indicates a simple renormalization procedure⁸ which provides an improved estimate. The electronic energy is a smooth function of D and the parameter k or Z in the v_{ext} potential. There exists an effective value of the parameter, denoted k_∞ or Z_∞ , for which the scaled energy at $D \rightarrow \infty$ is the same as for $D=3$ with the actual value of the parameter. The effective or renormalized values are evaluated from

$$\epsilon_\infty(k_\infty \text{ or } Z_\infty) = \epsilon_3(k \text{ or } Z), \quad (31)$$

where the scaled energy ϵ_D is the ratio of the total energy to that obtained with the electron-electron repulsion omitted, $Dk^{1/2}$ for the HL model and $[2Z/(D-1)]^2$ for the two

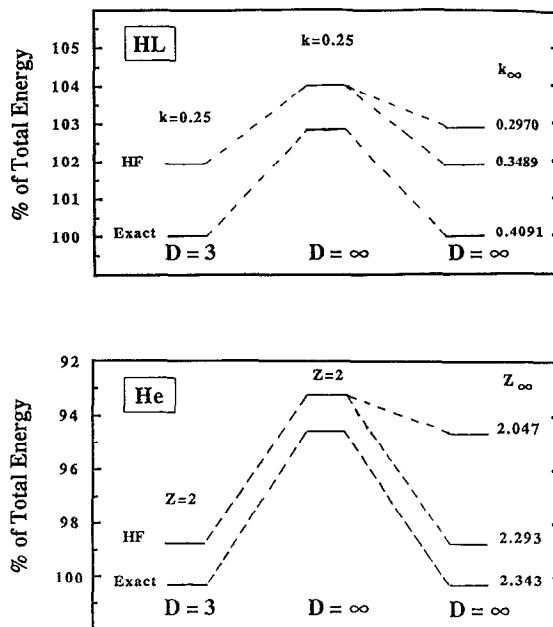


FIG. 6. Renormalization procedure applied to oscillator force constant k for HL model (upper panel) and to nuclear charge Z for the He atom (lower panel). At left are shown exact and Hartree-Fock energies for $D=3$. In the middle are corresponding energies for $D \rightarrow \infty$ limit. At right are energies derived from Eq. (30) by adjusting the force constant or nuclear charge to find the value for which the $D \rightarrow \infty$ limit will coincide with the $D=3$ energy.

electron atom. This gives $k_\infty = 0.40912\dots$ for the HL model (with $k=\frac{1}{4}$) and $Z_\infty = 2.343$ for the He atom (with $Z=2$), respectively. Thus, to offset the enhanced centrifugal repulsion of the $D \rightarrow \infty$ limit, the attraction to the nucleus must be enhanced, by increasing the effective spring constant for the HL model or the effective charge for the He atom.

This exact evaluation of k_∞ and Z_∞ is only of descriptive interest, since it requires knowledge of the $D=3$ energy. However, we can obtain a good approximation to the effective parameter value by using the $D \rightarrow \infty$ limit together with the HF results. By adjusting the parameter to make the HF energy at $D \rightarrow \infty$ match that at $D=3$, we find $k_\infty^{\text{HF}} = 0.3489$ and $Z_\infty^{\text{HF}} = 2.293$. To make an approximate allowance for the lack of correlation energy in the HF we augment these values by the increments needed to make the HF result coincide with the exact energy for $D \rightarrow \infty$ and thus reduce the correlation energy to zero in that limit. In this way we obtain effective values of $k^* = 0.39596$ and $Z^* = 2.3430$. The corresponding energies evaluated for the $D \rightarrow \infty$ limit then provide the renormalized estimates for the $D=3$ results: 2.00140 for the HL model and -2.90298 for the He atom. Compared with the exact energies, these values are, respectively, too high by 0.07% and by 0.026% (whereas k^* is low by 3.2% and Z^* low by 1.3%). On subtracting the HF energies for $D=3$ from these renormalized energies, we obtain for the correlation energy, -0.03779 for the HL model and -0.0417 for the He atom, respectively. These values are in error by -3.5% and -2%, respectively. It is encouraging that such results

TABLE IV. Comparison of correlation energies.

Species	Exact	BLYP	BP	RDS
He	-0.0420	-0.0416	-0.044	-0.0417
Li ⁺	-0.0435	-0.0438	-0.045	-0.0438
Be ⁺²	-0.0443	-0.0442	-0.049	-0.0447
HL ($k=\frac{1}{4}$)	-0.0392	-0.0351	-0.0538	-0.0377

can be attained merely by exploiting the simple $D \rightarrow \infty$ limit.

VI. DISCUSSION

The Hooke's Law model offers instructive comparisons with actual atoms as well as tests for approximate methods. In particular, as illustrated in Table IV, the correlation energy for the HL model resembles that for TEA but appears to afford a more stringent test of the density functional (BLYP or BP) and renormalized dimensional scaling (RDS) results. For the atoms, the BLYP and RDS results are within $\pm 1\%$, the BP within 4–11 %, but all three results are less good for the HL model.

Our comparisons thus far pertain to the analytically solvable case with $k=\frac{1}{4}$. The exact HL wave function of Eq. (4) then takes the form of a product of one-particle functions times a correlation factor linear in r_{12} . The differences between HL and TEA properties stem chiefly from the one-particle functions. A factor linear in r_{12} accounts for much of the correlation both in TEA, as found long ago by Hylleraas,¹⁰ and in many-electron atoms and molecules, as shown in extensive studies by Kutzelnigg.³¹ However, the HL model with $k=\frac{1}{4}$ does not provide an optimal comparison with atoms. As seen in Fig. 1, the range of densities spanned for $k=\frac{1}{4}$ is much lower than that for the He atom. From Eq. (7) we find the maximum HL density is given by

$$\rho(r=0; k=\frac{1}{4}) = N_0^2 [4 + \frac{7}{4}(2\pi)^{1/2}] = 0.089 504. \quad (32)$$

In terms of

$$r_s \equiv \left(\frac{4\pi}{3} \rho \right)^{-1/3},$$

the radius of a sphere containing one electron, this corresponds to 1.387 bohr units, and the density-averaged sphere radius is $\langle r_s \rangle = 2.44$ bohr. Thus for $k=\frac{1}{4}$ the HL density and functions pertain to a domain ($r_s > 1.4$) that corresponds to the low side of the "intermediate" density range for an electron gas.³² This is appropriate for the outer portions of large atoms or typical interstitial charge density in metals.⁵

Figure 7 shows the variation of $\langle r_s \rangle$ with the HL oscillator frequency, $\omega_0 = k^{1/2}$, and with the corresponding TEA parameter, $\omega_0 = Z^2$, as derived in the Appendix. Except for the hydride ion, the appropriate domain for small atoms is the higher density region with $\langle r_s \rangle \sim 1$, which corresponds to $k \sim 10$ or larger. The numerical calculations for the HL model^{12,13} extend well below and above this range. Figure 8 compares the dependence on ω_0 for the HL and TEA total energy and correlation energy. For $D=3$

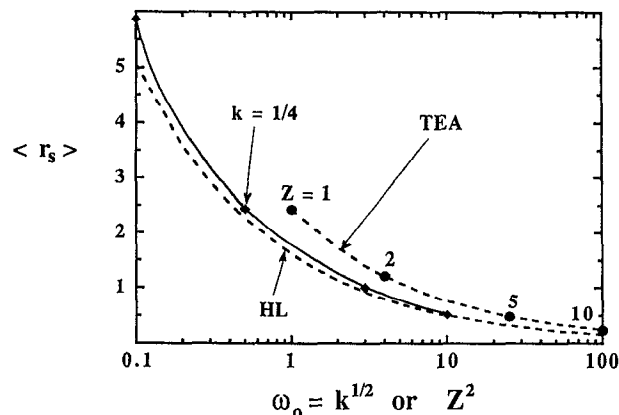


FIG. 7. Variation of average radius of a sphere containing one electron, $\langle r_s \rangle = \langle [(4\pi/3)\rho]^{-1/3} \rangle$, with parameter $\omega_0 = k^{1/2}$ or Z^2 for the HL model and for two-electron atoms. Solid curve fitted to HL points obtained from Eq. (7) for $k=\frac{1}{4}$ and from Ref. 12 for $k=10^{-2}$, 10, and 100. Dashed curves (derived in Appendix) show HL and TEA radii when electron-electron repulsion terms are omitted.

the HL results are from Ghosh and Samanta,¹³ augmented for large k by a perturbation expansion given by White and Brown,¹¹ the TEA data are from standard sources.³³ For $D \rightarrow \infty$ we derived the curves from Eq. (30) and the analogous TEA results.⁸ Despite the major difference in the

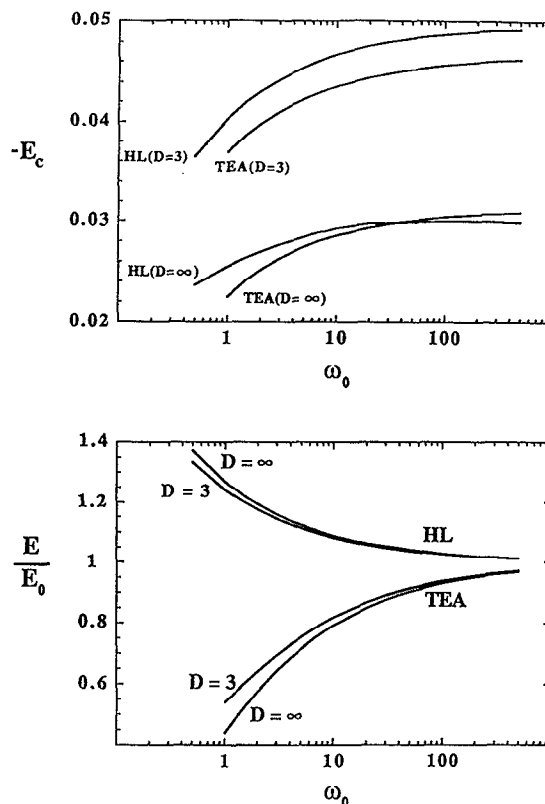


FIG. 8. Variation with parameter ω_0 of normalized total energy E/E_0 and correlation energy E_c for the HL model ($E_0 = 3\omega_0$) and TEA ($E_0 = \omega_0$). For the HL model, $\omega_0 = k^{1/2}$ is the vibrational frequency; for the two-electron atom, $\omega_0 = Z^2$.

nucleus-electron attraction terms, apparent in the total energies, the HL and TEA correlation energies are roughly parallel as functions of $\omega_0 = k^{1/2}$ or Z^2 . Electron-electron repulsion becomes relatively less important as ω_0 is increased and, hence, $\langle r_s \rangle$ decreased, but the correlation energy grows in absolute magnitude.

The ratio of the density gradient to density is important for many applications, as emphasized recently by Lacks and Gordon.³⁴ This is conveniently characterized by a dimensionless parameter,

$$s \equiv \frac{|\nabla\rho|}{2\rho k_f}, \quad (33)$$

where $k_f \equiv (3\pi^2\rho)^{1/3}$ is the local Fermi vector. From Eq. (7) we find the average value is $\langle s \rangle = 1.14$ for the HL ($k = \frac{1}{4}$) model. As shown in the Appendix, when electron-electron repulsion is omitted, $\langle s \rangle$ is independent of ω_0 ; we obtain $\langle s \rangle = 1.02$ and 3.30 for the HL and TEA cases, respectively.

Although our tests of the approximate BLYP or BP functionals in Figs. 2–4 pertain to the domain $r_s > 1.4$, the discrepancies have the same systematic character as those seen at lower r_s for other approximate functionals.¹² These errors are damped out to a large extent in the energies, as in Table II, but become prominent in the potentials, which are functional derivatives of the energy functionals. For the exchange potentials the errors are roughly tenfold larger than for the correlation potentials. This emphasizes the notorious difficulty of the quest for improved exchange-correlation potentials.^{4,12} Another awkward aspect, not encountered for TEA or HL ground states, stems from the marked conceptional differences between HF and density functional theory (DFT). Since correlation is defined with reference to the HF approximation, DFT cannot unequivocally separate exchange and correlation effects.³⁵

Yet DFT offers the great advantage that with efficient implementation the computational cost is comparable to the HF method.³⁶ For computations employing N atomic orbital basis functions, the rate-limiting step for DFT scales only as $O(N^2)$, just as for HF; this is the cost of handling the Coulomb integrals. The DFT cost for the correlation energy can be reduced to only $O(N)$ which, for large systems, is far less than for configuration interaction, Moller–Plesset perturbation theory, or other current *ab initio* methods.

DFT seems likely to be improved by dimensional scaling. The basic virtue of such scaling is that in the large D limit the magnitude, nature, and number of strong dynamical interactions become much less troublesome than usual. Accurately linking this limit to $D=3$ is often feasible because the dimension dependence of many-body effects tends to be mild when calibrated by appropriate one- or few-body problems.⁸ Here we have considered only the $D \rightarrow \infty$ limit, where both exact and HF results can be evaluated exactly for any atom or molecule as well as for the HL model. We have employed renormalization⁸ to illustrate how this limit can be usefully related to $D=3$. As seen in Fig. 7, the curves for $E_c(\omega_0; D=3)$ and $E_c(\omega_0; D \rightarrow \infty)$ are more nearly parallel for the atoms than

for the HL model. Nonetheless, in both cases the simple renormalization method gives quite good results.

Other means must be developed in order to incorporate the large dimension limit in constructing functionals or evaluating quantities besides the total energy or the correlation energy. Perturbation expansions⁸ in powers of $1/D$ might enable such an approach. Even for many-particle systems, the HF large dimension limit corresponds simply to setting all interparticle angles equal to 90° , so a dimensional perturbation expansion for DFT might provide a useful way to uncouple exchange from correlation. Such $1/D$ expansions may also be feasible for two-particle density functionals. As seen in Figs. 1 and 5, exchange and correlation effects are not prominent in the one-particle densities which depend only on the radial coordinate. In contrast, as seen in Table III, the interelectron angle for $D \rightarrow \infty$ directly reflects the extent of correlation. For heuristic analysis as well as computation, many aspects of DFT invite use of dimensional scaling.

ACKNOWLEDGMENTS

We have enjoyed instructive discussions of density functionals with John Loeser, and renormalization with Stella Sung. We are grateful for support received from the Office of Naval Research.

APPENDIX: DENSITIES WITHOUT ELECTRON REPULSION

In Figs. 1 and 7 and following Eq. (33) of the text, we give results obtained from very simple approximate HL and TEA density functions, $\rho_0(r)$, that omit electron-electron repulsion. These functions are specified in the caption of Fig. 1, where $\omega_0 = k^{1/2}$ or Z^2 . The average $r_s \equiv [(4\pi/3)\rho]^{-1/3}$, the radius of a sphere containing one electron, is given by

$$r_s = \left(\frac{4\pi}{3}\right)^{-1/3} \frac{\int_0^\infty \rho^{2/3} r^2 dr}{\int_0^\infty \rho r^2 dr} \quad (A1)$$

and we find

$$\langle r_s \rangle_{\text{HL}} = \frac{3^{7/6} \pi^{1/6}}{2^{5/2} \omega_0^{1/2}} = \frac{1.603}{\omega_0^{1/2}}, \quad (A2)$$

$$\langle r_s \rangle_{\text{TEA}} = \frac{3^{10/3}}{16 \omega_0^{1/2}} = \frac{2.434}{\omega_0^{1/2}}. \quad (A3)$$

One way to relate the HL force constant to the TEA nuclear charge is to make these $\langle r_s \rangle$ values agree. This yields $k = 0.1879Z^4$, corresponding to $k = 0.2, 3$, and 15 for $Z = 1, 2$, and 3, respectively.

For the gradient-to-density ratio of Eq. (33) we find $s_{\text{HL}} = \omega_0 r k_f^{-1}$ and $s_{\text{TEA}} = \omega_0^{1/2} k_f^{-1}$, with $k_f = (9\pi/4)^{1/3} 3r_s^{-1} = 3.093\rho^{1/3}$. Averaging as in Eq. (A1) gives

$$\langle s \rangle_{\text{HL}} = \frac{3^{5/3}}{2^{7/3} \pi^{1/6}} = 1.023, \quad (A4)$$

$$\langle s \rangle_{\text{TEA}} = \frac{4\pi^{1/3}}{3^{4/3}} \omega_0^{1/2} \langle r_s \rangle = 3.296. \quad (A5)$$

These quantities are constants, not dependent on ω_0 but only on the form of the density function.

- ¹E. Clementi, *Modern Techniques in Computational Chemistry* (ESCOM Science, Leiden, 1990).
- ²I. Shavitt, in *Advanced Theories and Computational Approaches to the Electronic Structure of Molecules*, edited by C. E. Dykstra (Reidel, Dordrecht, 1984), pp. 185–196.
- ³J. P. Dahl and J. Avery, *Local Density Approximation in Quantum Chemistry and Solid State Physics* (Plenum, New York, 1984).
- ⁴N. H. March and B. M. Deb, *The Single Particle Density in Physics and Chemistry* (Academic, New York, 1987).
- ⁵R. G. Parr and W. Yang, *Density Functional Theory of Atoms and Molecules* (Oxford University, London, 1989).
- ⁶R. G. Gordon and R. LeSar, *Adv. Quantum Chem.* **21**, 341 (1990).
- ⁷W. Kohn and L. J. Sham, *Phys. Rev. A* **140**, 1133 (1965).
- ⁸*Dimensional Scaling in Chemical Physics*, edited by D. R. Herschbach, J. Avery, and O. Goscinski (Kluwer, Dordrecht, 1992).
- ⁹C. E. Wulfman, *J. Chem. Phys.* **33**, 1567 (1960).
- ¹⁰N. R. Kestner and O. Sinanoglu, *Phys. Rev.* **128**, 2687 (1962).
- ¹¹R. J. White and W. B. Brown, *J. Chem. Phys.* **53**, 3869, 3880 (1970).
- ¹²P. M. Laufer and J. B. Krieger, *Phys. Rev. A* **33**, 1480 (1986).
- ¹³A. Samanta and S. K. Ghosh, *Phys. Rev. A* **42**, 1178 (1990); **43**, 6395 (1991); S. K. Ghosh and A. Samanta, *J. Chem. Phys.* **94**, 517 (1991).
- ¹⁴S. Kais, D. R. Herschbach, and R. D. Levine, *J. Chem. Phys.* **91**, 7791 (1989).
- ¹⁵From BLYP optimal density; computed with code of Ref. 16 using functional of Ref. 19.
- ¹⁶R. D. Amos, I. L. Alberts, J. S. Andrew, S. M. Colwell, N. C. Handy, D. Jayaklaka, P. J. Knowles, R. Kobayashi, N. Koga, K. E. Laidig, P. E. Maslen, J. E. Rice, J. Sanz, E. D. Simandiras, A. J. Stone and M. D. Su. CADPACS: The Cambridge Analytic Derivatives Package, University of Cambridge, 1992.
- ¹⁷J. P. Perdew, R. G. Parr, M. Levy, and J. L. Balduz, *Phys. Rev. Lett.* **49**, 1691 (1982).
- ¹⁸C. W. Murray, G. J. Laming, N. C. Handy, and R. D. Amos, *Chem. Phys. Lett.* **199**, 551 (1992).
- ¹⁹C. Lee, W. Yang, and R. G. Parr, *Phys. Rev. B* **37**, 785 (1988); A. D. Becke, *Phys. Rev. A* **38**, 3098 (1988).
- ²⁰R. Colle and O. Salvetti, *Theor. Chem. Acta* **37**, 329 (1975).
- ²¹S. H. Vosko, L. Wilk, and M. Nusair, *Can. J. Phys.* **58**, 1200 (1980).
- ²²D. M. Ceperly and B. J. Alder, *Phys. Rev. Lett.* **45**, 566 (1980).
- ²³J. P. Perdew, *Phys. Rev. B* **33**, 8822 (1986).
- ²⁴D. C. Langreth and M. J. Mehl, *Phys. Rev. B* **28**, 1809 (1983).
- ²⁵J. G. Loeser, Z. Zhen, S. Kais, and D. R. Herschbach, *J. Chem. Phys.* **95**, 4525 (1991).
- ²⁶R. Gordon and Y. S. Kim, *J. Chem. Phys.* **56**, 3122 (1972).
- ²⁷J. G. Loeser and D. R. Herschbach, *J. Phys. Chem.* **89**, 3444 (1985); *J. Chem. Phys.* **86**, 3512 (1987).
- ²⁸D. Z. Goodson and D. R. Herschbach, *J. Chem. Phys.* **86**, 4997 (1987).
- ²⁹M. López-Cabrera, A. L. Tan, and J. G. Loeser, *J. Phys. Chem.* **97**, 2467 (1993).
- ³⁰J. Avery, D. Z. Goodson, and D. R. Herschbach, *Theor. Chem. Acta* **82**, 1 (1991).
- ³¹W. Klopper and W. Kutzelnigg, *J. Chem. Phys.* **94**, 2020 (1991), and work cited therein.
- ³²W. J. Carr, *Phys. Rev.* **122**, 1437 (1961).
- ³³E. Clementi, *J. Chem. Phys.* **38**, 2248 (1963); **39**, 175 (1963).
- ³⁴D. J. Lacks and R. G. Gordon, *J. Chem. Phys.* (to be published).
- ³⁵M. Cook and M. Karplus, *J. Phys. Chem.* **91**, 31 (1987).
- ³⁶B. G. Johnson, P. M. W. Gill, and J. A. Pople, *J. Chem. Phys.* **97**, 7846 (1992).